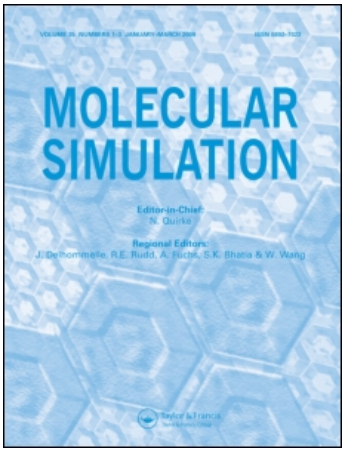

Molecular Simulation
Publication details, including instructions for authors and subscription information:
http://www.informaworld.com/smpp/title~content=t713644482

Shear viscosity of ionic liquids from non-equilibrium molecular dynamics simulation

Jan Picálek[a]; Jiří Kolafa[a]
[a] Department of Physical Chemistry, Prague Institute of Chemical Technology, Praha, Czech Republic

To cite this Article Picálek, Jan and Kolafa, Jiří(2009) 'Shear viscosity of ionic liquids from non-equilibrium molecular dynamics simulation', Molecular Simulation, 35: 8, 685 — 690
To link to this Article: DOI: 10.1080/08927020802680703
URL: http://dx.doi.org/10.1080/08927020802680703

Molecular Simulation
Vol. 35, No. 8, July 2009, 685–690

Taylor & Francis
Taylor & Francis Group

Shear viscosity of ionic liquids from non-equilibrium molecular dynamics simulation

Jan Picálek and Jiří Kolafa*

Department of Physical Chemistry, Prague Institute of Chemical Technology, Praha, Czech Republic

(*Received 3 September 2008; final version received 3 December 2008*)

Temperature dependence of viscosity of butyl-3-methylimidazolium hexafluorophosphate is investigated by non-equilibrium molecular dynamics simulations with cosine-modulated force in the temperature range from 360 to 480 K. It is shown that this method is able to correctly predict the shear viscosity. The simulation setting and choice of the force field are discussed in detail. The all-atom force field exhibits a bad convergence and the shear viscosity is overestimated, while the simple united atom model predicts the kinetics very well. The results are compared with the equilibrium molecular dynamics simulations. The relationship between the diffusion coefficient and viscosity is examined by means of the hydrodynamic radii calculated from the Stokes–Einstein equation and the solvation properties are discussed.

Keywords: room temperature ionic liquids; viscosity; non-equilibrium molecular dynamics; solvation; imidazolium

1. Introduction

Ionic liquids (IL), more precisely 'room-temperature ionic liquids', are salts liquid at ambient or moderately elevated temperatures. They are usually composed of organic cations and inorganic or less frequently organic anions [1]. The cations are typically imidazolium or pyridinium based, with one or more alkyl substituents. Anions comprise halide ions, tetrafluoroborate (BF_4^-), tetrachloroaluminate ($AlCl_4^-$), hexafluorophosphate (PF_6^-) or bis(perfluoromethyl-sulfonyl)imide anion (Tf_2N^-). Properties that make IL so attractive are negligible vapour pressure, thermal stability, non-inflammability and the ability to dissolve simultaneously in both organic and inorganic substances. Their quite rapid emergence as alternative solvents has involved a rapidly growing number of scientific publications and examples of application. The most extensively studied family of ionic liquids has been that of the 1-alkyl-3-methylimidazolium cation with anions PF_6^-, BF_4^- and Tf_2N^-. Frequently measured bulk properties include density [2–5], viscosity [2,4–11], heat capacity [3], self-diffusivity [2,4,5,12], ionic conductivity [2,4,5], etc. The earliest calculations performed on this family of pure ionic liquids included quantum calculations [13–16], MD simulation [17–26] and also some MC [27,28] simulations. For the purposes of classical simulations, a number of force fields have been developed [18–28].

In this work, a non-equilibrium molecular dynamics (NEMD) was used to investigate the temperature dependence of viscosity of relatively highly viscous $BMIMPF_6$ in the temperature range from 360 to 480 K. The NEMD is a standard method to determine shear viscosities and has been extensively applied to simple fluids or more rarely to polar liquids. Several authors have investigated the shear viscosity of molten alkali halides via NEMD [29,30]. Hu and Margulis [31] performed NEMD of 1-hexyl-3-imidazolium chloride ionic liquid using extremely large simulation boxes.

Viscosity is usually calculated from equilibrium molecular dynamics (EMD), which is often (but not always [32]) considered more accurate. Shear viscosity estimates from EMD simulation have been reported for 1,3-dimethylimidazolium chloride [33], 1-ethyl-3-methylimidazolium chloride [34,35], 1-ethyl-3-methylimidazolium hexafluorophosphate [35] and 1-ethyl-3-methylimidazolium nitrate [26]. Although the EMD simulations on systems such as high-temperature molten salts or solvents like water predicted the dynamical behaviour well, the complex nature of ionic liquids requires extremely long runs with large number of ions [31,36]. Difficulties related to ionic liquids' EMD simulations motivated this study to employ the NEMD to access their shear viscosity. We employ the most straightforward classical NEMD algorithm [37] in which the system responds by a velocity profile to a modulated shear force. It thus complements the very recent work on 1-butyl-3-methylimidazolium hexafluorophosphate ($BMIMPF_6$) [38] using similar strategy called there 'reverse NEMD'.

Finally, the hydrodynamic radii of ions are computed from the Stokes–Einstein equation. Required self-diffusion coefficients are taken from our previous EMD work [36].

*Corresponding author. Email: jiri.kolafa@vscht.cz

ISSN 0892-7022 print/ISSN 1029-0435 online

DOI: 10.1080/08927020802680703
http://www.informaworld.com

2. Theory

2.1 Stokes–Einstein law

Let us consider a spherical solute of radius r_i immersed in a homogeneous Newtonian fluid of shear viscosity η. Then its diffusion coefficient is related to fluid viscosity by the Stokes–Einstein law [39],

$$D_i = \frac{kT}{6\pi\eta r_i}, \tag{1}$$

where k is the Boltzmann constant and T is the temperature. Since a real solvent is not a homogeneous Newtonian fluid and a real solute is not a hard sphere, r_i defined by Equation (1) is called the hydrodynamic radius. By definition, the hydrodynamic radius r_i reflects both the solvent and shape (dynamic) effects. Therefore, its size (compared with the solute size) can tell us about solvation, conformation of the solute, etc.

2.2 Viscosity from shear stress simulations

Our NEMD algorithm is a standard (but to some extent forgotten) method [37]. The simulation is performed in a rectangular box of sizes $L_x \times L_y \times L_z$, where $L_x = L_y$ and $L_z = 3L_x$. External acceleration acting on particles in the direction perpendicular to the z-axis is

$$a_i = C_\mathrm{f} \cos\left(\frac{2\pi z_i}{L_z}\right). \tag{2}$$

We use forces in the direction of diagonal (1,1,0). This small modification of standard set-up (1,0,0) was motivated by a less regular pattern of nearest images in the direction of applied force. Then

$$f_{x,i} = f_{y,i} = K_\mathrm{f} m_i \cos\left(\frac{2\pi z_i}{L_z}\right), \tag{3}$$

where $K_\mathrm{f} = C_\mathrm{f}/\sqrt{2}$. In practical implementation, we also add a small z-force to all atoms so that the sum of forces over all atoms is exactly zero (it slightly deviates because particles are not distributed ideally uniformly). The Navier–Stokes equation [40] for a steady Newtonian flow of an incompressible fluid reads as

$$\eta\nabla^2\vec{v} + \vec{f} = 0, \tag{4}$$

where $\vec{f}$ is the (averaged) external force per unit volume, $|\vec{f}| = f = \rho C_\mathrm{f}$, v is the velocity, and $\rho = \sum_i m_i/V$ is the mass density. Its solution is a steady flow proportional to the applied force. Systematic contribution to the (thermal) velocities of individual atoms is then

$$v_i = C_\mathrm{v} \cos\frac{2\pi z_i}{L_z}, \tag{5}$$

where

$$\eta = \left(\frac{L_z}{2\pi}\right)^2 \rho \frac{C_\mathrm{f}}{C_\mathrm{v}}. \tag{6}$$

In order to calculate C_v and consequently η, we define the sums

$$S_\mathrm{f} = \sum_i f_{x,i} \cos\frac{2\pi z_i}{L_z}, \tag{7}$$

$$S_\mathrm{p} = \sum_i (v_{x,i} + v_{y,i}) \cos\frac{2\pi z_i}{L_z} \tag{8}$$

and the final formula for viscosity adopts the form

$$\eta = \rho \frac{L_z^2}{2\pi^2} \frac{\langle S_\mathrm{f}\rangle}{\langle S_\mathrm{p}\rangle}. \tag{9}$$

During simulation, also the velocity amplitude

$$C_\mathrm{v} = \frac{S_\mathrm{f}}{S_\mathrm{p}} \frac{C_\mathrm{f}}{2} \tag{10}$$

is monitored to check for the steady-state condition.

Heating rate is an important control quantity in the simulation. In the steady-state flow, it is

$$\dot{E} = \frac{\mathrm{d}E}{\mathrm{d}t} = \frac{1}{2}\int \eta(\nabla v)^2 dV = \frac{V}{\eta}\left(\frac{C_\mathrm{f}\rho L_z}{4\pi}\right)^2. \tag{11}$$

It is useful to express it via expected increase in temperature because it will help us to set up the thermostat used to remove the heat. The crudest estimate of the isochoric heat capacity is that of the ideal gas, $C_\mathrm{v} = N_\mathrm{f} k/2$, where N_f is the number of degrees of freedom of the simulation box. Then

$$C_\mathrm{f} = \sqrt{\frac{8\pi^2 \dot{T}\eta N_\mathrm{f} k}{V L_z^2 \rho^2}}. \tag{12}$$

In addition, we use the Berendsen thermostat to remove the friction heat. This thermostat adds to the Newton equations of motion a friction-like term proportional to $(T - T_\mathrm{kin})$ $\mathbf{v}$, where we define $(1/2)kT_\mathrm{kin} = (1/2)\Sigma_i m_i[\boldsymbol{v}_i - \boldsymbol{v}(z_i)]^2$, i.e. the macroscopic component of the velocity $\boldsymbol{v}(z_i)$ is subtracted (although this component is well within the noise for the lowest friction forces used). The thermostat coupling is expressed via correlation time τ_T (exactly, an ideal gas system would relax exponentially with this correlation time).

For larger systems, it takes some time until a steady velocity profile develops. Relaxation to this steady state

is exponential with the correlation time given by

$$\tau_v = \frac{\rho}{\eta}\left(\frac{L_z}{2\pi}\right)^2. \quad (13)$$

As soon as an estimate of viscosity is known, the recommended strategy to reach the stationary state as fast as possible is to simulate time $t = \tau_v \ln 2$ with doubled parameter $\xi = \dot{T}\eta$ and half τ_T.

2.3 Error estimation

The main source of errors is quantity S_p. For small shear forces, it fluctuates around zero. Its time behaviour is governed by correlations with correlation time τ_v. Long correlations make standard methods for error estimations unreliable. However, the time correlation function of S_p has a typical shape of damped oscillations, which can help us to determine the error in average $\langle S_p \rangle$ with higher reliability. We fit the time correlation function of S_p to formula

$$\mathrm{Cov}(S_p(t), S_p(t+k))/\mathrm{Var}(S_p) = \cos(Ak)\exp(-Bk) \quad (14)$$

and the error is then

$$\delta S_p = \sqrt{\frac{\mathrm{Var}(S_p) + 2\sum_{i=1}^{\infty}\mathrm{Cov}(S_p(t), S_p(t+i))}{m-1}}, \quad (15)$$

where m is the number of measurements. Finally, at low temperatures the error δS_p is comparable to $\langle S_p \rangle$; the viscosity is obtained by division. We therefore provide the viscosity errors as estimated bounds at the 68% confidence level.

2.4 Fluid anisotropy via cross section

Molecules under high shear stress try to orient in parallel to the shear force and thus to diminish their cross section and in turn the viscosity. While for small elongated molecules the orientation of the molecular axis can be monitored, no such axis is defined for molecules of complex shape like $BMIM^+$. We therefore determine the cross section directly. To do this, a molecule is replaced by fused hard spheres of radii given by $R_i + R_{He}$, where R_i is the van der Waals radius of the atom and $R_{He} = 1.4$ Å. The cross section is calculated by projecting such a molecule to a plane and counting matching points in a rectangular grid of span 1 Å. The cross sections in three perpendicular directions, (1,1,0), (1, −1,0) and (0,0,1), are monitored.

3. Simulation details

Non-equilibrium molecular dynamics simulations were performed by package MACSIMUS (http://www.vscht.cz/fch/software/macsimus). Two different force fields were used for comparison purposes. They will be denoted UA and AA in what follows, and are taken from [23,24], respectively. The simulations were carried out in the NVT ensemble using the Berendsen thermostat at temperatures ranging from 360 to 480 K. The rectangular box was used, the ratio of dimensions was set to $L_x{:}L_y{:}L_z = 1{:}1{:}3$. The simulations were performed with 250 cations and 250 anions, the box dimension was chosen to match the experimental density in the temperature range of interest [2,41]. We consider these dimensions sufficient because the NEMD results by Hu and Margulis [31] on 8232 ion pairs of 1-hexyl-3-imidazolium chloride gave similar results like the small ones.

The initial configuration was a lattice with a low density and ions were placed randomly at the vertices. The box size was gradually rescaled so that the system reached the desired estimated bulk density. The system was intensively cooled during this part of simulation, but for final equilibration and production run the thermostat correlation time was set to 1 ps. Equilibration time was 200 ps, after that production runs lasting at least 7 ns were started. Equations of motion were integrated by the Verlet algorithm [37], the time step in the simulations was 1.0 fs. The Lennard-Jones cut-off was set to 14 Å, the long-range Coulombic interactions were handled with the Ewald summation method [37].

3. Results and discussion

All calculated shear viscosities are along with the estimated SEs listed in the Table 1 and plotted in Figure 1. The computed self-diffusion coefficients from EMD simulation [36] are listed in the Table 2 at temperatures 360 and 380 K.

It is seen that the united atom force field gives viscosities in a good agreement with the experiment while the all-atom values are off by almost an order of magnitude; only the temperature dependence is qualitatively correct. The disagreement witnesses about an

Table 1. Shear viscosity of $BMIMPF_6$ computed using force fields by Liu et al. [24] and Urahata and Ribeiro [23], and listed in the left and right column, respectively; heating rate is given by the Equation (12).

T (K)	Viscosity (UA force field; mPa s)	Viscosity (AA force field; mPa s)
360	31.3 ± 6.2	231.3 ± 97.2
380	17.2 ± 2.7	142.8 ± 44.3
400	9.1 ± 0.8	58.5 ± 17.5
420	6.9 ± 0.5	39.0 ± 13.7
440	4.9 ± 0.3	19.3 ± 7.6
460	3.6 ± 0.2	14.2 ± 3.5
480	2.8 ± 0.1	9.3 ± 2.0

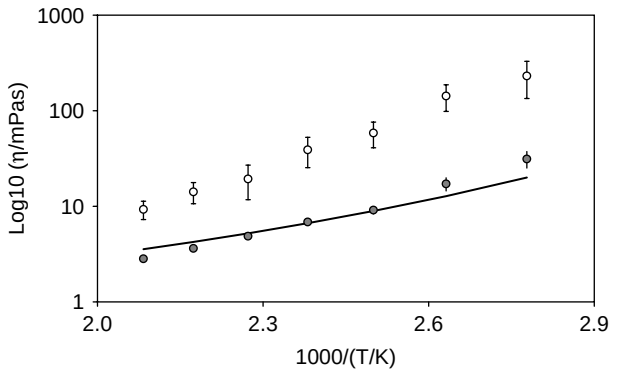

Figure 1. The shear viscosity of $BMIMPF_6$; open circles: all-atom force field [24], full circles: united atom force field [23], line: experimental values [4].

inappropriate force field; the same phenomenon has been observed for diffusivities [36]. The recent NEMD results obtained by very long runs at a smaller temperature 300 K [38] arrived at a good agreement with experiment, but the used force field was different [42].

An important question is whether the usual pair additive non-polarisable force field is suitable to model ionic liquids. Inclusion of polarisability was found to be critical for an accurate of simple inorganic salts [43,44] as well as of alkyl nitrates [45].

Yan et al. [26] developed a polarisable model of 1-ethyl-3-methylimidazolium nitrate and discussed the influence of polarisability on bulk properties. The influence of polarisability was found to be important but not crucial. However, in our recent study, the interfacial behaviour of water/$BMIMBF_4$ solution was reproduced by a polarisable force field only [46]. Several authors performed MD simulations of imidazolium-based ILs using non-polarisable force field and discussed the possible influence of polarisability [31,47,48]. Nevertheless, there is no other work dealing with polarisable force field of $BMIMPF_6$ we can compare with.

Reliable calculation of viscosities requires careful setting of the force, expressed by the parameter ξ; the force constant is proportional to $\xi^{1/2}$. That is why we ran several sets of simulations with different values of ξ. The higher ξ, the larger systematic error; the lower ξ, the larger statistical error. The calculated viscosities at large heating rates are always underestimated because the molecules are reoriented along the force vector, which diminishes the friction force. This effect is worse at low temperatures. We assess it to be the impact using cross sections of the $BMIM^+$ cation. At the lowest temperature, the lowest heating rate, and the all-atom force field (the worst case), the cross section is 85.6 $Å^2$ in the direction of the force (1,1,0), 86.0 $Å^2$ in (1, −1,0), and 86.1 $Å^2$ in the direction of the z-axis. The respective maximum values (maximum anisotropy at extremely high heating rates) are 75, 86 and 93. Thus, at the lowest heating rate, the anisotropy is only about 3% of the maximum, which is acceptable. The systematic error for the united-atom force field is smaller.

In order to guarantee good statistics, the lowest temperature for our computations was set to 360 K; at lower temperatures, the correlation times become comparable to our simulation times (7 ns). The maximum of the temperature range (480 K) is below the decomposition temperature [49]. Because of heat production in NEMD simulations, the quality and properties of a thermostat is crucial. The averaged kinetic temperature $\langle T_{\mathrm{kin}} \rangle$ differs from the thermostat value T, but for friction forces used in production runs the difference is 0.03 K or less. Kinetic temperatures calculated from molecular centres-of-mass only and from velocities with respect to the centres-of-mass (internal motions and rotations) are another quality tests of the integration, constraint dynamics and thermostat; they match within combined error bars (of 1–2 K). For these reasons, we expect that the selected Berendsen thermostat used in this work should be satisfactory. The pressure in the NVT ensemble with density set to the experimental one was typically about 10 and 100 MPa for the all-atom and united-atom force field, respectively. We therefore simulated selected systems in the NpT ensemble for comparison; however, no significant difference from the NVT results was found.

Finally, we used the calculated viscosities to calculate the hydrodynamic radii of $BMIMPF_6$; the self-diffusion coefficients were taken from EMD simulation [36]. The experimental values are based on the viscosities and diffusivities by Tokuda et al. [4]. The results (see Table 3) are somehow controversial and their interpretation is not easy.

The experimental hydrodynamic radii of ions are smaller than their geometric radii (5.2 Å for the cation and 4.1 Å for the anion, based on the respective cross sections).

Table 2. Diffusivity of $BMIMPF_6$ [4] and MD results [36] computed using force fields by Urahata and Ribeiro (UA) [23] and Liu et al. (AA) [24].

	Experimental		UA force field		AA force field	
T (K)	D_{CATION} (10^{-11} m^2 s^{-1})	D_{ANION} (10^{-11} m^2 s^{-1})	D_{CATION} (10^{-11} m^2 s^{-1})	D_{ANION} (10^{-11} m^2 s^{-1})	D_{CATION} (10^{-11} m^2 s^{-1})	D_{ANION} (10^{-11} m^2 s^{-1})
360	8.5	6.9	2.16 ± 0.44	1.23 ± 0.3	0.76 ± 0.28	0.42 ± 0.09
380	14	12	4.91 ± 0.58	2.08 ± 0.39	0.89 ± 0.24	0.52 ± 0.11

Table 3. Hydrodynamic radii of the cations $BMIM^+$ and anions PF_6^- computed using force fields by Liu et al. (AA) [24] and Urahata and Ribeiro (UA) [23].

	Experimental		UA force field		AA force field	
T (K)	r_{CATION} (Å)	r_{ANION} (Å)	r_{CATION} (Å)	r_{ANION} (Å)	r_{CATION} (Å)	r_{ANION} (Å)
360	1.54	1.90	3.90	6.85	1.50	2.71
380	1.56	1.87	3.30	7.79	2.19	3.75

This means that the simple model of a sphere in a Newtonian fluid is inaccurate (which is not surprising for such a complex liquid). The ions move faster (larger diffusivity) than they would in a Newtonian continuum. One can imagine ions hopping sneakily between local potential minima in a more slowly changing network of ion pairs (viscosity is a collective phenomenon), or locally lower viscosity; we shall see below that the latter explanation may be more relevant.

The hydrodynamic radii obtained from the UA force field are nevertheless close to the geometric ones; in other words, the fluid around ions composed of smooth united atoms seems to be almost Newtonian even at short separations. Even though the values of both diffusivity and viscosity are in a good agreement with the experiment than for the AA force field, the oversimplified UA force field gives worse hydrodynamic radii.

The viscosity of the AA model increases more dramatically than the diffusivity drops and consequently the radii decrease as well and are in a good agreement with the experimental values than in the UA case. In spite of wrong magnitudes, the AA model is able to capture the structure of the ionic liquid better than the UA does.

It remains to discuss the inequality $r_{cation} < r_{aniion}$ (or equivalently $D_{cation} > D_{anion}$) which is correctly predicted by both models, while the opposite inequality is for the valid geometric radii (even if the cation is viewed along its elongated axis). The smaller radius of the cation reflects its larger diffusivity and lower local viscosity. It might be attributed to its neighbourhood composed of smaller anions.

4. Conclusions

In this work, we calculated the viscosity of $BMIMPF_6$ over a temperature range of 360–480 K. We used a NEMD method based on applying a cosine-modulated shear force and observing the velocity profile. This method is based only on formulas of continuum mechanics, and is therefore very close to the real experiment. We concentrated on the simulation setting and choice of the force field. The employed united atom force field predicts the shear viscosity very well, the all-atom force field gives only qualitatively correct temperature dependence. In addition, the all-atom force field exhibits a bad convergence and also other properties show 'slow kinetics'. Consequently, for advances in this area, the force field should be improved by polarisability, replacing too rigid Lennard-Jones terms by exp-6 (Buckingham or Busing) potentials and by careful setting of all parameters.

Acknowledgements

We gratefully acknowledge a support from the Czech Science Foundation (project 203/07/1006) and the computing facilities from the Czech Ministry of Education (Center for Biomolecules and Complex Molecular Systems, project LC512).

References

[1] F. Endres and S.Z.E. Abedin, *Air and water stable ionic liquids in physical chemistry*, Phys. Chem. Chem. Phys. 8 (2006), pp. 2101–2116.
[2] A. Noda, K. Hayamizu, and M. Watanabe, *Pulsed-gradient spin-echo ^1H and ^{19}F NMR ionic diffusion coefficient, viscosity, and ionic conductivity of non-chloroaluminate room-temperature ionic liquids*, J. Phys. Chem. B 105 (2001), pp. 4603–4610.
[3] C.P. Fredlake, J.M. Crosthwaite, D.G. Hert, S.N.V.K. Aki, and J.F. Brennecke, *Thermophysical properties of imidazolium-based ionic liquids*, J. Chem. Eng. Data 49 (2004), pp. 954–964.
[4] H. Tokuda, K. Hayamizu, K. Ishii, A.H. Susan, and M. Watanabe, *Physicochemical properties and structures of room temperature ionic liquids. 1. Variation of anionic species*, J. Phys. Chem. B 108 (2004), pp. 16593–16600.
[5] H. Tokuda, K. Hayamizu, K. Ishii, A.H. Susan, and M. Watanabe, *Physicochemical properties and structures of room temperature ionic liquids. 2. Variation of alkyl chain length in imidazolium cation*, J. Phys. Chem. B 109 (2005), pp. 6103–6110.
[6] O.O. Okoturo and T.J. VanderNoot, *Temperature dependence of viscosity for room temperature ionic liquids*, J. Electroanal. Chem. 568 (2004), pp. 167–181.
[7] K.R. Seddon, A. Stark, and M. Torres, *The influence of chloride, water and organic solvents on the physical properties of ionic liquids*, Pure Appl. Chem. 12 (2000), pp. 2275–2287.
[8] J.G. Huddleston, A.E. Visser, H.D. Willauer, and R.D. Rogers, *Characterization and comparison of hydrophilic and hydrophobic room temperature ionic liquids incorporating the imidazolium cation*, Green Chem. 3 (2001), pp. 156–164.
[9] H. Shirota and E. Castner, *Why are viscosities lower for ionic liquids with $-CH_2Si(CH_3)_3$ vs $-CH_2C(CH_3)_3$ substitutions on the imidazolium cations?*, J. Phys. Chem. B 46 (2005), pp. 21576–21585.
[10] H. Shirota and E. Castner, *Physical properties and intermolecular dynamics of an ionic liquid compared with its isoelectronic neutral binary solution*, J. Phys. Chem. A 42 (2005), pp. 9388–9392.
[11] E. Gomez, B. Gonzalez, A. Dominguez, E. Tojo, and J. Tojo, *Physical properties of pure 1-ethyl-3-methylimidazolium ethylsulfate and its binary mixtures with ethanol and water at several temperatures*, J. Chem. Eng. Data 51 (2006), pp. 696–701.
[12] T. Umecky, M. Kanakubo, and Y. Ikushima, *Self-diffusion coefficients of 1-butyl-3-methylimidazolium hexafluorophosphate with pulsed-field gradient spin-echo NMR technique*, Fluid Phase Equilibr. 228 (2005), pp. 329–333.
[13] Z. Meng, A. Dolle, and W.R. Carper, *Gas phase model of an ionic liquid: semi-emperical and* ab initio *bonding and molecular structure*, J. Mol. Struct. 585 (2002), pp. 119–128.

[14] E.R. Talaty and S. Raja, *Raman and infrared spectra and* ab initio *calculations of C2-4MIM imidazolium hexafluorophosphate ionic liquids*, J. Phys. Chem. B 108 (2004), pp. 13177–13184.
[15] N.E. Heimer, R.E. Del Sesto, and W.R. Carper, *Evidence for spin diffusion in a H,H-NOESY study of imidazolium tetrafluoroborate ionic liquid*, Magn. Reson. Chem. 42 (2004), pp. 71–75.
[16] R.W. Berg, M. Deetlefs, K.R. Seddon, I. Shim, and J.M. Thompson, *Raman and* ab initio *studies of simple and binary 1-alkyl-3-methylimidazolium ionic liquids*, J. Phys. Chem. B 109 (2005), pp. 19018–19025.
[17] S. Urahata and M. Ribeiro, *Collective excitations in an ionic liquid*, J. Chem. Phys. 124 (2006), 074513.
[18] C.G. Hanke, S.L. Price, and R.M. Lynden-Bell, *Intermolecular potentials for simulations of liquid imidazolium salts*, Mol. Phys. 99 (2001), pp. 801–809.
[19] J. Andrade, E.S. Böes, and H. Stassen, *A force field for liquid state simulations on room temperature molten salts: 1-Ethyl-3-methyl-imidazolium tetrachloroaluminate*, J. Phys. Chem. B 106 (2002), pp. 3546–3548.
[20] T.I. Morrow and E.J. Maginn, *Molecular dynamics study of the ionic liquid 1-*n*-butyl-3-methylimidazolium hexafluorophosphate*, J. Phys. Chem. B 106 (2002), pp. 12807–12813.
[21] C.J. Margulis, H.A. Stern, and B.J. Berne, *Computer simulation of a 'green chemistry' room-temperature ionic solvent*, J. Phys. Chem. B 106 (2002), pp. 12017–12021.
[22] J.N.C. Lopes, J. Deschamps, and A.H. Padua, *Modeling ionic liquids using a systematic all-atom force field*, J. Phys. Chem. B 108 (2002), pp. 2038–2047.
[23] S.M. Urahata and M.C. Ribeiro, *Structure of ionic liquids of 1-alkyl-3-methylimidazolium cations: A systematic computer simulation study*, J. Chem. Phys. 120 (2004), pp. 1855–1863.
[24] Z. Liu, S. Huang, and W. Wang, *Refined force field for molecular simulation of imidazolium-based ionic liquids*, J. Phys. Chem. B 108 (2004), pp. 12978–12989.
[25] S.U. Lee, J. Jung, and H. Young-Kyu, *Molecular dynamics study of the ionic conductivity of 1-*n*-butyl-3-methylimidazolium salts as ionic liquids*, Chem. Phys. Lett. 406 (2005), pp. 332–340.
[26] T. Yan, C.J. Burnham, M.G. Del Popolo, and G.A. Voth, *Molecular dynamics simulation of ionic liquids: the effect of electronic polarizability*, J. Phys. Chem. B 108 (2004), pp. 11877–11881.
[27] J.K. Shah, J.F. Brennecke, and E.J. Maginn, *Thermodynamic properties of the ionic liquid 1-*n*-butyl-3-methylimidazolium hexafluorophosphate from Monte Carlo simulations*, Green Chem. 4 (2002), pp. 112–118.
[28] J.K. Shah and E.J. Maginn, *A Monte Carlo simulation study of the ionic liquid 1-*n*-butyl-3-methylimidazolium hexafluorophosphate: liquid structure, volumetric properties and infinite dilution solution thermodynamics of CO_2*, Fluid Phase Equilibr. 222 (2004), pp. 195–203.
[29] J. Delhommelle and J. Petravic, *Shear viscosity of molten sodium chloride*, J. Chem. Phys. 118 (2003), pp. 2783–2791.
[30] N. Galamba, N. de Castro, and J.F. Ely, *Shear viscosity of molten alkali halides from equilibrium and nonequilibrium molecular dynamics simulations*, J. Chem. Phys. 122 (2005), 224501.
[31] Z. Hu and C.J. Margulis, *On the response of an ionic liquid to external perturbations and the calculation of shear viscosity*, J. Phys. Chem. B 111 (2006), pp. 4705–4714.
[32] B. Hess, *Determining the shear viscosity of model liquids from molecular dynamics simulations*, J. Chem. Phys. 116 (2002), pp. 209–217.
[33] B.L. Bhargava and S. Blasubramanian, *Dynamics in a room-temperature ionic liquid: A computer simulation study of 1,3-dimethylimidazolium chloride*, J. Chem. Phys. 123 (2005), 144505; *Erratum*, J. Chem. Phys. 125 (2006), 219901.
[34] C. Rey-Castro and L.F. Vega, *Transport properties of the ionic liquid 1-ethyl-3-methylimidazolium chloride from equilibrium molecular dynamics simulation. The effect of temperature*, J. Phys. Chem. B 110 (2006), pp. 14426–14435; *Erratum*, J. Phys. Chem. B 110 (2006), p. 16157.
[35] Y. Shim, M.Y. Choi, and H.J. Kim, *A molecular dynamics computer simulation study of room-temperature ionic liquids. II. Equilibrium and nonequilibrium solvation dynamics*, J. Chem. Phys. 122 (2005), 044511.
[36] J. Picálek and J. Kolafa, *Molecular dynamics study of conductivity of ionic liquids: The Kohlrausch law*, J. Mol. Liquids 134 (2007), pp. 29–33.
[37] M.P. Allen and D. Tildesley, *Computer Simulation of Liquids*, Clarendon Press, Oxford, 1987.
[38] Z. Wei, F. Leroy, S. Balasubramanian, and F. Müller-Plathe, *Shear viscosity of the ionic liquid 1-*n*-butyl 3-methylimidazolium hexafluorophosphate* [*bmim*][PF_6] *computed by reverse non-equilibrium molecular dynamics*, J. Phys. Chem. B 112 (2008), pp. 8129–8133.
[39] P.W. Atkins, *Physical Chemistry*, W.H. Freeman & Company, New York, 1990.
[40] A.D. Polyanin, A.M. Kutepov, A.V. Vyazmin, and D.A. Kazenin, *Hydrodynamics, Mass and Heat Transfer in Chemical Engineering*, Taylor & Francis, London, 2002, p. 2.
[41] Z. Gu and J.F. Brennecke, *Volume expansivities and isothermal compressibilities of imidazolium and pyridinium based ionic liquids*, J. Chem. Eng. Data 47 (2002), pp. 339–345.
[42] B.L. Bhargava and S.J. Balasubramanian, *Refined potential model for atomistic simulations of ionic liquid* [*bmim*][PF_6], J. Chem. Phys. 127 (2007), 114510.
[43] R.J. Heaton, R. Brookes, P.A. Madden, M. Salanne, C. Simon, and P. Turq, *A first-principles description of liquid BeF_2 and its mixtures with LiF: 1. Potential Development and Pure BeF_2*, Phys. Chem. B 110 (2006), pp. 11454–11460.
[44] Y.C. Lee, J. Kolafa, L.A. Curtiss, M.A. Ratner, and D.F. Shriver, *Molten salt electrolytes. I. Experimental and theoretical studies of LiI/$AlCl_3$*, J. Chem. Phys. 114 (2001), pp. 9998–10009.
[45] O. Borodin and G.D. Smith, *Structure and dynamics of* N*-methyl-*N*-propylpyrrolidinium bis(trifluoromethanesulfonyl)imide ionic liquid from molecular dynamics simulations*, J. Phys. Chem. B 110 (2006), pp. 11481–11490.
[46] J. Picálek, B. Minofar, J. Kolafa, and P. Jungwirth, *Aqueous solutions of ionic liquids: Study of the solution/vapor interface using molecular dynamics simulations*, Phys. Chem. Chem. Phys. 10 (2007), pp. 5765–5775.
[47] B.L. Bhargava, S. Balasubramanian, and M.L. Klein, *Modelling room temperature ionic liquids*, Chem. Commun. 29 (2008), pp. 3339–3351.
[48] Y. Shim, J. Duan, M.Y. Choi, and J. Kim, *Solvation in molecular ionic liquids*, J. Chem. Phys. 119 (2003), pp. 6411–6414.
[49] N.L. Ngo, K. LeCompte, L. Hargens, and A.B. McEwen, *Thermal properties of imidazolium ionic liquids*, Therm. Acta 357 (2000), pp. 97–102.